Kinetics of CO Substitution in Reactions of η^3-Cyclopropenyl Complexes of Iron, Cobalt, Rhodium, and Iridium with Phosphorus Ligands. First Examples of a Dissociative Mechanism for CO Substitution in the Cobalt Triad Carbonyl Complexes

Jian-Kun Shen,† David S. Tucker,‡ Fred Basolo,*,† and Russell P. Hughes*,‡

Department of Chemistry, Northwestern University, Evanston, Illinois 60208-3113, and Burke Chemistry Laboratory, Dartmouth College, Hanover, New Hampshire 03755-3564

Received March 29, 1993⊗

Abstract: Kinetic studies of the substitution reactions of $M(\eta^3\text{-}C_3{}^tBu_3)(CO)_3$ (M = Co, Rh, Ir) with triethyl phosphite provide the first examples of dissociative CO substitution for carbonyl complexes of the cobalt triad. Rates are first-order in the concentrations of the complexes and zero-order in the concentrations of the phosphite; high $\Delta H^\ddagger$ and large positive $\Delta S^\ddagger$ values and CO retardation of the rate are also consistent with a dissociative mechanism. At high temperature and low phosphite concentrations, the rate of reaction (M = Co) shows a nonlinear dependence on ligand concentrations, due to competition between the entering ligand and CO for the coordinatively unsaturated active intermediate; the same results were observed for the reaction of $Co(\eta^3\text{-}C_3{}^tBu_3)(CO)_3$ with $P(^nBu)_3$. The equilibrium constants of the reactions were also measured. Despite the differences in basicities of these ligands, the equilibrium constants increase with decreasing size of the ligands. A plot of ln K vs cone angles of the ligands shows a good linear relationship between the two, implying that the stabilities of the monosubstituted complexes are predominantly determined by steric effects of the ligand. The large ligands PPh_3 or $P(c\text{-}C_6H_{11})_3$ do not react with the cobalt complex. Dissociative CO substitution of $Rh(\eta^3\text{-}C_3{}^tBu_3)(CO)_3$ is much faster relative to the Co and Ir compounds than is the rate of associative CO substitution of $Rh(\eta^5\text{-}C_5H_5)(CO)_2$ relative to the Co and Ir counterparts. For the first time a comparison of the rates of CO dissociation from a Co triad system with the relative rates of CO dissociation from other transition metal triads is made. Reaction of $Fe(\eta^3\text{-}C_3{}^tBu_3)(CO)_2(NO)$ with $P(^nBu)_3$ gives only the monosubstituted product by two simultaneous dissociative and associative pathways. A bent-NO mechanism is favored for the associative pathway. Reaction of $Fe(\eta^3\text{-}C_3Ph_3)(CO)_2(NO)$ with $P(^nBu)_3$ gives both CO substitution and ring-expansion products, whereas the reaction of $Fe(\eta^3\text{-}C_3Ph_3)(CO)_2(NO)$ with PPh_3 follows only a dissociative pathway to yield monosubstituted product with a rate constant the same as k_1 obtained from the reaction with $P(^nBu)_3$. Detailed mechanistic discussions are presented.

Introduction

Ligand hapticity changes that generate an open coordination site have become important fundamental components of certain organometallic reactions. In particular associative reaction mechanisms made possible by such hapticity changes have been established for CO substitution reactions of metal carbonyls containing polyolefin and polyenyl ligands.[1] Kinetic studies have been carried out on CO substitution reactions of cyclopentadienyl,[2] indenyl,[3] trindene,[4] allyl,[5] and heterocycle[6] metal carbonyl complexes. By changing their coordination mode from $\eta^n \rightarrow \eta^{n-2}$, these ligands allow an 18-electron metal complex to undergo CO substitution by an associative mechanism. A mechanistically similar, though topologically quite different, effect is observed in CO substitution reactions of complexes that contain NO as an ancillary ligand. Reversible transformation of the NO ligand from a linear to bent configuration opens up a coordination site and facilitates an associative substitution mechanism. The reactions of $Co(CO)_3(NO)$[7a] and $Fe(CO)_2(NO)_2$[7b] with tertiary phosphorus ligands (L) to give $Co(CO)_2(NO)L$ and $Fe(CO)(NO)_2L$, respectively, are thoroughly studied examples of the latter phenomenon.

The simplest cyclic enyl ring ligand is the η^3-cyclopropenyl ligand, which could conceivably undergo ring-slippage from $\eta^3 \rightarrow \eta^1$ in the same fashion as observed for its acyclic allyl analogue,[5] yet no kinetic investigations have been reported on CO substitution reactions of cyclopropenylmetal carbonyl complexes.

Cyclopropenyl ligands are known to bind to transition metal centers via η^1-, η^2- and η^3-coordination.[8-12] Unfortunately the reactions of most carbonyl complexes containing the η^3-cyclopropenyl moiety with exogenous ligands do not afford the simple product(s) of CO substitution. Instead, facile cyclopropenyl migration to coordinated CO and subsequent ring expansion to afford oxocyclobutenyl complexes often competes with ligand substitution. For example, reactions of the (η^3-triphenylcyclopropenyl)iron complex **1a** (Chart I) with some tertiary phosphorus ligands lead to both CO substitution to give **2a** and ring expansion to afford **3**.[11] However, analogous reactions of the η^3-tri-*tert*-butylcyclopropenyl analogue **1b** yields only the CO substitution product **2b**.[11] These reactions could proceed via associative mechanisms involving $\eta^3 \rightarrow \eta^1$ slippage of the cyclopropenyl ring

† Northwestern University.
‡ Dartmouth College.
⊗ Abstract published in *Advance ACS Abstracts*, October 15, 1993.

(1) (a) Basolo, F. *Polyhedron* **1990**, *9*, 1503. (b) O'Connor, J. M.; Casey, C. P. *Chem. Rev.* **1987**, *87*, 307.
(2) Schuster-Woldan, H. G.; Basolo, F. *J. Am. Chem. Soc.* **1966**, *88*, 1657.
(3) Rerek, M. E.; Basolo, F. *Organometallics* **1983**, *2*, 372; *J. Am. Chem. Soc.* **1984**, *106*, 5908.
(4) Bang, H.; Lynch, T. J.; Basolo, F. *Organometallics* **1992**, *11*, 40.
(5) Palmer, G. T.; Basolo, F. *J. Am. Chem. Soc.* **1985**, *107*, 3122.
(6) Kershner, D. L.; Basolo, F. *Coord. Chem. Rev.* **1989**, *79*, 279.
(7) (a) Thorsteinson, E. M.; Basolo, F. *J. Am. Chem. Soc.* **1966**, *88*, 3929; *Inorg. Chem.* **1966**, *5*, 1691. (b) Morris, D. E.; Basolo, F. *J. Am. Chem. Soc.* **1968**, *90*, 2536.
(8) Gompper, R.; Bartmann, E.; Noth, H. *Chem. Ber.* **1979**, *112*, 218.
(9) McClure, M. D.; Weaver, D. L. *J. Organomet. Chem.* **1973**, *54*, C59.
(10) Olander, W. K.; Brown, T. L. *J. Am. Chem. Soc.* **1972**, *94*, 2139.
(11) Hughes, R. P.; Lambert, J. M. J.; Hubbard, J. L. *Organometallics* **1986**, *5*, 797.
(12) Hughes, R. P.; Lambert, J. M. J.; Whitman, D. W.; Hubbard, J. L.; Henry, W. P.; Rheingold, A. L. *Organometallics* **1986**, *5*, 789.

0002-7863/93/1515-11312$04.00/0

Chart I

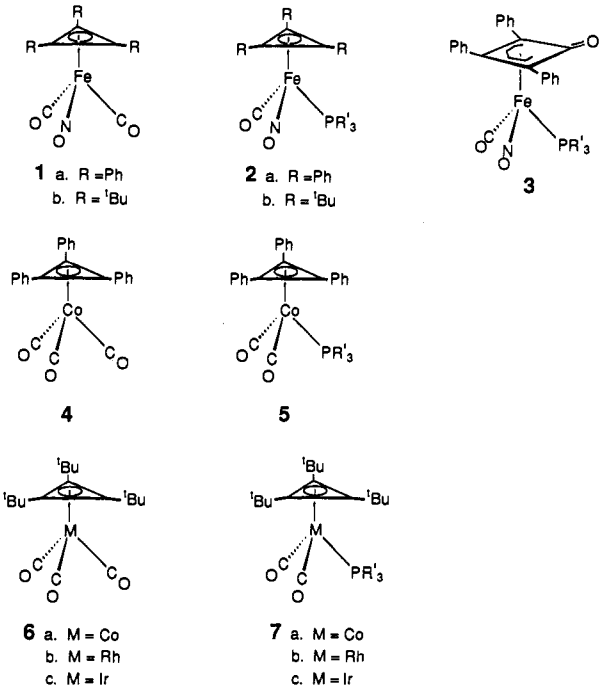

or by a linear to bent NO transformation, but no kinetic studies of this reaction had previously been reported. Similar ring expansion is also observed in the reactions of cyclopropenyl cations with other transition-metal carbonyl anions.[12] In contrast to the iron complex **2a**, reaction of the isoelectronic cobalt analogue **4** with PMe_3 affords only the substitution product **5**. In this latter case, the absence of an NO ligand limits any associative pathway to slippage of the cyclopropenyl ligand. In this paper we report the results of kinetic studies of these CO substitution and ring expansion reactions.

The preparation of the series of complexes $M(\eta^3\text{-}C_3{}^tBu_3)(CO)_3$ (**6**) (M = Co, Rh, Ir), the molecular structure determination of the iridium complex, synthetic studies of some of their CO substitution reactions, and dynamic NMR studies of the barriers to cyclopropenyl rotation are all described elsewhere.[13] Earlier, photoelectron spectroscopy studies on the cobalt and iridium complexes revealed that the metal centers are best considered as d^{10} centers, i.e., M(–I) centers η^3-bound to a cyclopropenyl cation.[14] This picture is similar to that for the nitrosyl complex $Co(CO)_3(NO)$.[14] The reactions of this series of cobalt triad metal complexes with tertiary phosphorus ligands afford only CO substitution products **7**,[13] providing an opportunity to study the effect of variation of the metal on the substitution kinetics. It is well-known that, for organometallic compounds, the 2nd row transition metal complex of a given triad is generally the most substitution labile.[1] This was found to be true for the cobalt triad compounds $(\eta^5\text{-}C_5H_5)M(CO)_2$ (M = Co, Rh, Ir), which react by an associative mechanism involving slippage of the cyclopentadienyl ring.[2] Indeed all kinetic data on CO substitution of mononuclear metal carbonyls of the cobalt triad show associative reaction mechanisms, although the replacement of THF from Co(CO)L(THF)(NO) proceeds by a dissociative process.[15] However, the rates of dissociative ligand substitution from the iron triad $M(CO)_5$ (M = Fe, Ru, Os)[16] and from the nickel triad $M[P(OEt)_3]_4$ (M = Ni, Pd, Pt)[17] increase for the transition metals in the order 1st row < 3rd row < 2nd row.

We were interested whether the mechanism of CO substitution in complexes **6** would also prove to be associative, strongly implicating a ring-slippage mechanism analogous to that in their cyclopentadienyl relatives. Here we report results of a detailed kinetic study of CO substitution in this series of complexes. Results reported here show that CO substitutions of the tri-*tert*-butylcyclopropenyl metal complexes **6** proceed by a dissociative mechanism, making it possible to compare and discuss the generality of these results with the reactivities known for other transition metal triads.

Experimental Section

Reagents. $Co(C_3{}^tBu_3)(CO)_3$ (**6a**),[12] $Rh(C_3{}^tBu_3)(CO)_3$ (**6b**),[13] $Ir(C_3{}^tBu_3)(CO)_3$ (**6c**),[14] $Fe(C_3{}^tBu_3)(CO)_2(NO)$ (**2b**),[12] and $Fe(C_3Ph_3)(CO)_2(NO)$ (**2a**)[12] were prepared according to literature methods. $P(OEt)_3$ and $P(^nBu)_3$ were refluxed over sodium and distilled under nitrogen atmosphere. PPh_3 were recrystallized from ethyl alcohol. Toluene and decalin were predried and distilled from Na/benzophenone before use. All manipulations of solutions for kinetic studies were carried out under an atmosphere of N_2, using standard Schlenk techniques.

Kinetic Studies. All kinetic experiments were run under pseudo-first-order conditions, with the concentration of entering nucleophile in 10-fold excess or more than that of complex concentrations (1 or 3×10^{-3} M). Kinetic data were obtained by following the disappearances of CO stretching bands of reactant complexes. The infrared spectra were obtained on a Nicolet 5PC FT-IR spectrometer using either a cell with 0.2-mm NaCl windows or, in the case of Rh complex, a special P/N 20.500 variable-temperature IR cell with 0.5-mm AgCl windows. Constant temperatures (for temperature above 50 °C) were obtained using a Cole-Parmer DiGi-Sense temperature controller with a type J thermocouple. This system was able to maintain temperatures within +0.2 °C. For temperatures below 50 °C and above –14 °C, a Neslab RTE-8 refrigeration circulating bath was used for constant-temperature control. Temperatures below –14 °C were obtained by using CCl_4/CO_2 (–23 °C) and CH_3CN/CO_2 (–42 °C) baths. Plots of ln A vs time were linear over 2 half-lives ($r^2 > 0.995$) for all the reactions. The slope of these lines yield observed rate constants. The second-order rate constants were obtained from the slope of the lines calculated by the least-squares method for plots of k_{obsd} vesus concentration of ligand, while first-order rate constants were obtained from the intercepts of the same lines with the k_{obsd} axis. Correlation coefficients of least-squares plots ($R^2 > 0.995$) were good. In cases where the metal complexes did not exhibit second-order rate constants, the first-order rate constants were obtained directly from the average values of k_{obsd} for reactions at the same temperature. Activation parameters were calculated by the least-squares method from the plot of $\ln(k/T)$ versus $1/T$.

CO Retardation. The CO substitution reaction of $Co(\eta^3\text{-}C_3{}^tBu_3)(CO)_3$ (**6a**) with $P(OEt)_3$ was kinetically studied under 1 atm of CO at 90.6 °C. In a 100-mL flask, 3 mL of reaction solution with 0.16 M of $P(OEt)_3$ was added under N_2 atmosphere. The solution was then frozen, and N_2 was pumped out. The solution was raised to room temperature under a flow of CO gas which was conducted into the hood. The rate for the reaction is not first-order in the concentration of the complex; instead, it became slower as more reactant converted to the product and almost reached equilibrium with 60% of the reactant complex converted to the monosubstituted complex.

Equilibrium Constant Measurement. The equilibrium constants were measured at 101 °C for reactions of $Co(\eta^3\text{-}C_3{}^tBu_3)(CO)_3$ (**6a**) with different phosphorus ligands. The reactions were taken with starting $Co(\eta^3\text{-}C_3{}^tBu_3)(CO)_3$ concentration at 2.82×10^{-3} M and at 0.1 atm of CO mixed with N_2. The ligand concentrations changed from 0.015 M to 0.8 M for different phosphines or phosphites, in order to get accurate measurements of complex concentrations. Selected experiments show that K values obtained are repeatable with 15% error limits.

Isolation of the Kinetic Products. The solutions from kinetic runs for the reaction of $Ir(\eta^3\text{-}C_3{}^tBu_3)(CO)_3$ (**6c**) with $P(OEt)_3$ in toluene were collected. The solvent was removed under vacuum, and the residue was extracted with pentane. The solution was then concentrated and cooled to –78 °C. The compound $Ir(\eta^3\text{-}C_3{}^tBu_3)(CO)_2[P(OEt)_3]$ was obtained as white crystals: FT-IR (toluene, cm^{-1}) 1993.4, 1943.7; ^1H NMR ($CDCl_3$) 3.87 ($P\text{-}CH_2$, 6H), 1.16–1.21 (36H); MS (*e/m*; % abundance) 623 (0.5), 622 (2.2), 621 (0.2), 620 (1.2) P^+, 595 (19.7), 594 (60.6), 593 (12.5), 592 (39.8) $P^+ - CO$, 549 (17.4) $P^+ - CO - OEt$, 454 (38.4) $P^+ - P(OEt)_3$, 207 (100) $C_3{}^tBu_3{}^+$.

(13) Hughes, R. P.; Tucker, D. S.; Rheingold, A. L. *Organometallics* **1993**, *12*, 3069.
(14) Lichtenberger, D. L.; Hoppe, M. L.; Subramanian, L.; Kober, E. M.; Hughes, R. P.; Hubbard, J. L.; Tucker, D. S. *Organometallics* **1993**, *12*, 2025.
(15) Zhang, S.; Dobson, G. R. *Inorg. Chem.* **1989**, *28*, 324.
(16) Shen, J. K.; Gao, Y. C.; Shi, Q. Z.; Basolo, F. *Inorg. Chem.* **1989**, *28*, 4304. Huq, R.; Poe, A. J.; Chawla, S. *Inorg. Chim. Acta* **1980**, *38*, 121.
(17) Meier, M.; Basolo, F.; Pearson, R. G. *Inorg. Chem.* **1969**, *8*, 795.

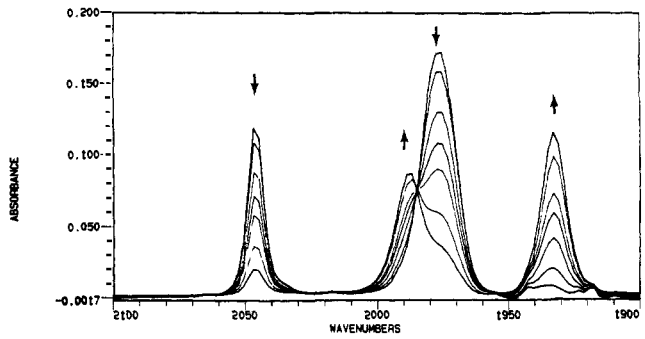

Figure 1. Infrared ν_{CO} absorbance changes vs time for reaction 1 (M = Co).

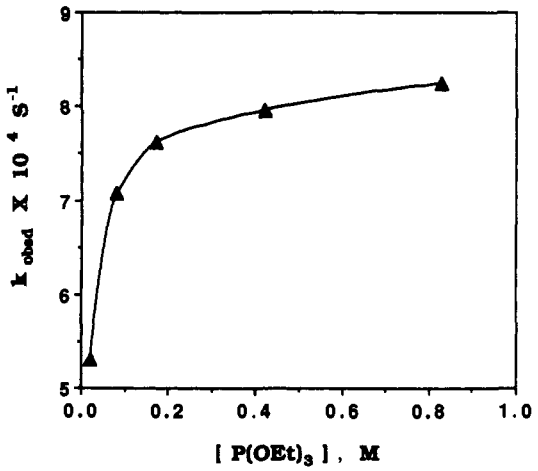

Figure 2. Plot of k_{obsd} vs ligand concentrations for reaction 1 (M = Co) at 101 °C.

$Co(C_3{}^tBu_3)(CO)_2[P(OEt)_3]$. This compound was isolated in the same way as that for the Ir analogue and was purified by crystallization from ethanol. FT-IR (toluene, cm^{-1}): 1987.5, 1932.8. ^1H NMR ($CDCl_3$): 3.92 (P–CH_2, 6H), 1.16–1.20 (36H). MS (*e/m*; % abundance) 488 (6.3) P^+, 461 (12.2), 460 (41.5) P^+ – CO, 433 (31.7), 432 (100) P^+ – 2CO, 207 (56.0) $C_3{}^tBu_3{}^+$. Detailed descriptions of the preparation and characterization of compounds of this type are given elsewhere.[13]

Results

$M(\eta^3\text{-}C_3{}^tBu_3)(CO)_3$ (6; M = Co, Rh, Ir). The reaction of $M(\eta^3\text{-}C_3{}^tBu_3)(CO)_3$ (M = Co, Rh, Ir) with $P(OEt)_3$ in toluene proceeded according to eq 1 to give monosubstituted products

$$M(\eta^3\text{-}C_3{}^tBu_3)(CO)_3 + P(OEt)_3 \rightarrow (\eta^3\text{-}C_3Bu^t{}_3)M(CO)_2[P(OEt)_3] + CO \quad (1)$$

$$M = Co, Rh, Ir$$

$M(\eta^3\text{-}C_3{}^tBu_3)(CO)_2[P(OEt)_3]$. Values of k_{obsd} were obtained by monitoring the decrease of the carbonyl bands of the starting metal carbonyls (Figure 1). The rates of the reactions (eq 1) are first-order in the concentrations of complexes. At higher temperature and low ligand concentrations, the rates for the reaction (M = Co) show a dependence on the ligand concentrations (Figure 2). The rates almost reach their limits when [P(OEt)$_3$]/[complex] = 50. This is due to the competition of CO with phosphite for the coordinatively unsaturated intermediate. First-order rate constants and activation parameters for the reactions (eq 1) are included in Table I. The CO substitution reactions of $M(\eta^3\text{-}C_3{}^tBu_3)(CO)_3$ with $P(^nBu)_3$ were also studied. The rate of the reaction became slower as the reaction proceeded. Plots of ln A_t vs time do not yield straight lines even for the first half-life of the reaction (Figure 3). No further attemp was made to estimate the rate constants for these reactions.

Table I. First-Order Rate Constants and Activation Parameters for Reactions of $M(\eta^3\text{-}C_3{}^tBu_3)(CO)_3$ (6) with $P(OEt)_3$ in Toluene

M	ν_{CO} (cm^{-1})	T (°C)	k_1 (s^{-1})	ΔH^* (kcal/mol)	ΔS^* (cal/mol·K)
Co (**6a**)	1976	79.5	4.15×10^{-5}		
	2046	90.6	1.91×10^{-4}		
		101.5	7.96×10^{-4}	34.4 ± 0.3	18.7 ± 0.8
Rh (**6b**)	1991	−14	2.7×10^{-2}		
	2055	−23	3.5×10^{-3}		
		−42	1.8×10^{-4}	22.4 ± 4.9	20.4 ± 17.9
Ir (**6c**)	1985	8.0	3.90×10^{-5}		
	2053	18.4	2.04×10^{-4}		
		29.1	1.05×10^{-3}	25.9 ± 0.4	13.5 ± 1.4

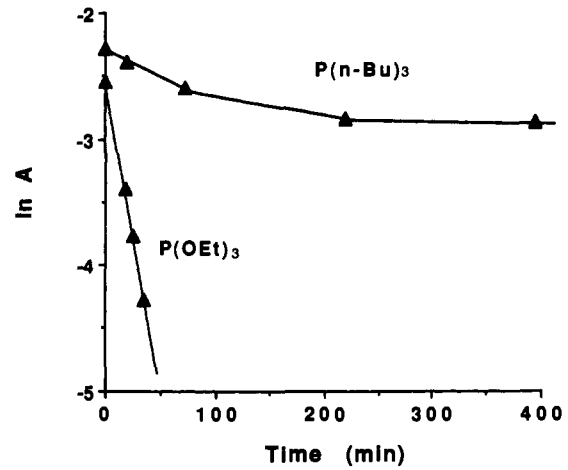

Figure 3. Plot of ln A_t vs time for the reactions of $Co(\eta^3\text{-}C_3{}^tBu_3)(CO)_3$ (**6a**) with $P(^nBu)_3$ (0.12 M) and with $P(OEt)_3$ (0.13 M) at 101.5 °C.

Table II. Equilibrium Constants for Reactions of $Co(\eta^3\text{-}C_3{}^tBu_3)(CO)_3$ (6a) with Different Ligands in Toluene at 101.0 °C

ligand	θ (deg)[a]	pK_a[a]	K (atm M^{-1})
1. $P(OCH_2)_3CCH_3$	101	1.74	70
2. $P(OMe)_3$	107	2.60	5.4
3. $P(OEt)_3$	109	3.31	6.5
4. $PPhMe_2$	122	6.50	0.51
5. $P(OPh)_3$	128	−2.0	0.15
6. $P(Et)_3$	132	8.69	0.055
7. PPh_2Me	136	4.57	0.017
8. PPh_3	145	2.73	NR[b]
9. PCy_3	170	9.70	NR[b]

[a] Reference 30. [b] No reaction.

Equilibrium Constants. Equilibrium constants were calculated using eq 2, where P_{CO} is constant (0.1 atm) during the reaction,

$$K = P_{CO}[\text{Co–ligand}]/[\text{ligand}][\text{Co–CO}] \quad (2)$$

[Co–CO] is the concentration of $Co(\eta^3\text{-}C_3{}^tBu_3)(CO)_3$ measured after the reaction has reached equilibrium, [Co–ligand] is the concentration of the product obtained from $[\text{Co–CO}]_{start}$ – [Co–CO], and [ligand] is the concentration of free ligand at equilibrium. The equilibrium constants for different ligands are included in Table II.

$Fe(\eta^3\text{-}C_3{}^tBu_3)(CO)_2(NO)$ (1b). The reaction of $Fe(\eta^3\text{-}C_3{}^tBu_3)(CO)_2(NO)$ with $P(^nBu)_3$ in decalin gives monosubstituted product (eq 3). Its CO stretching bands (Table III) are similar

$$Fe(\eta^3\text{-}C_3{}^tBu_3)(CO)_2(NO) + P(^nBu)_3 \rightarrow Fe(\eta^3\text{-}C_3{}^tBu_3)(CO)(NO)[P(^nBu)^3] + CO \quad (3)$$

$$k_{obsd} = k_1 + k_2[P(^nBu)_3] \quad (4)$$

Table III. Kinetic Products and Their CO and NO Stretching Frequencies

complex	IR (cm^{-1})
$Co(C_3{}^tBu_3)(CO)_2P(OEt)_3$[a]	1987, 1933
$Rh(C_3{}^tBu_3)(CO)_2P(OEt)_3$[a]	2002, 1955
$Ir(C_3{}^tBu_3)(CO)_2P(OEt)_3$[a]	1993, 1944
$Fe(C_3{}^tBu_3)(CO)(NO)P(^nBu)_3$[b]	1935 (CO), 1701 (NO)
$Fe(C_3Ph_3)(CO)(NO)PPh_3$[b]	1965 (CO), 1725 (NO)
$Fe(CO)(C_3Ph_3)(NO)P(^nBu)_3$[b]	1958 (CO), 1717 (NO)
$Fe(C_4Ph_3O)(CO)(NO)P(^nBu)_3$[b]	1990 (CO), 1754 (NO), 1680 (CO)
$Co(C_3Ph_3)(CO)_2P(^nBu)_3$[a]	1993, 1941

[a] In toluene. [b] In decalin.

Table IV. First-Order Rate Constants and Activation Parameters for Reactions of $Fe(\eta^3\text{-}C_3R_3)(CO)_2(NO)$ (1) with $P(^nBu)_3$ and Their CO and NO Stretching Frequencies in Decalin

R	IR (cm^{-1})	T (°C)	k_1 (s^{-1})	ΔH^* (kcal/mol)	ΔS^* (cal/mol·K)
^{t}Bu (**1b**)	2020 (CO)	74.0	3.25×10^{-6}		
	1969 (CO)	86.0	2.30×10^{-5}		
	1745 (NO)	96.0	6.75×10^{-5}	34.6 ± 4.8	15.8 ± 13.3
Ph (**1a**)	2034 (CO)	69.5	1.14×10^{-5}		
	1991 (CO)	81.5	5.95×10^{-5}		
	1757 (NO)	91.0	2.10×10^{-4}	31.4 ± 2.8	14.6 ± 1.4

Table V. Second-Order Rate Constants and Activation Parameters for the CO Substitution Reaction of $Fe(\eta^3\text{-}C_3{}^tBu_3)(CO_2(NO)$ (1b) with $P(^nBu)_3$ in Decalin

T (°C)	k_2 (s^{-1} M^{-1})	ΔH^* (kcal/mol)	ΔS^* (cal/mol·K)
74.0	4.62×10^{-6}		
86.0	2.00×10^{-5}		
96.0	5.89×10^{-5}	28.7 ± 0.6	−0.5 ± 1.7

to those of analogous compounds.[11,12] The kinetics of the reaction (eq 3) obeys a two-term rate law. This suggests the reaction (eq 3) occurs by simultaneous dissociative and associative pathways (eq 4). First-order and second-order rate constants and activation parameters for both pathways are included in Tables IV and V.

$Fe(\eta^3\text{-}C_3Ph_3)(CO)_2(NO)$ (1a). The reaction of $Fe(\eta^3\text{-}C_3Ph_3)(CO)_2(NO)$ with $P(^nBu)_3$ in decalin gives the monosubstituted compound $Fe(\eta^3\text{-}C_3Ph_3)(CO)(NO)P(^nBu)_3$ and ring-expanded oxocyclobutenyl product $Fe(\eta^3\text{-}C_4Ph_3O)(CO)(NO)P(^nBu)_3$ (eq 5). Their IR spectra in the 2200–1600-cm^{-1} region (Table III) are similar to those for analogous compounds.[11,12] The observed rate constant k_{obsd} obtained by monitoring the disappearance of starting metal carbonyl obeys a two-term rate law (eq 4). First-order and second-order rate constants are obtained from the intercepts and slopes of the plots of k_{obsd} versus concentrations of $P(^nBu)_3$ (Figure 4). These and activation parameters for each pathway are included in Tables IV and VI.

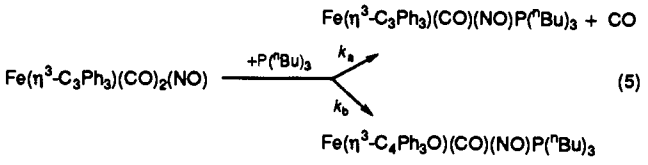

(5)

$Co(\eta^3\text{-}C_3Ph_3)(CO)_3$ (4). The reaction of $Co(\eta^3\text{-}C_3Ph_3)(CO)_3$ with $P(^nBu)_3$ only affords monosubstituted product. The rate for the CO substitution reaction obeys a first-order rate law. First-order rate constants and activation parameters are included in Table VII.

Discussion

Kinetics and Mechanism of CO Substitution Reactions of $M(\eta^3\text{-}C_3{}^tBu_3)(CO)_3$ (6; M = Co, Rh, Ir). The reactions of $M(\eta^3\text{-}C_3{}^tBu_3)(CO)_3$ (M = Co, Rh, Ir) with triethyl phosphite give monosubstituted products (eq 1). No ring expansion products were observed from IR spectra of reaction solutions after 3 half-lives. The rates of reaction (eq 1) are first-order in the concentrations of the complexes and zero-order in the concentrations of the phosphite. This suggests the reactions (eq 1) undergo dissociative mechanisms. High ΔH^* and large positive ΔS^* values (Table I) are consistent with a dissociative mechanism, as is also the CO retardation of the rates of reaction (Figure 5). Furthermore, at high temperature and low phosphite concentrations, the rate of reaction (eq 1; M = Co) shows a nonlinear dependance on ligand concentrations (Figure 2). This is believed to be due to a competition between the entering ligand and CO

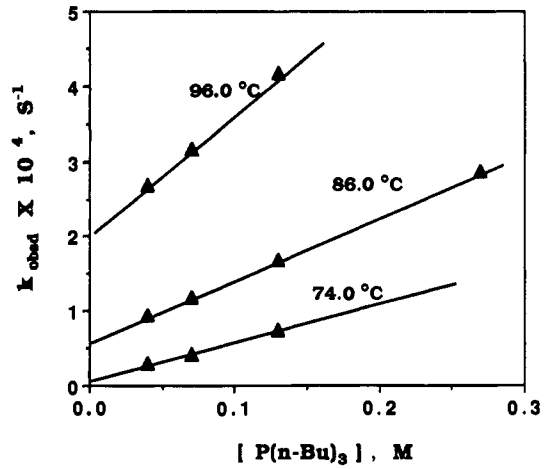

Figure 4. Plot of k_{obsd} vs ligand concentrations for the reaction of $Fe(C_3Ph_3)(CO)_2(NO)$ (**1a**) with $P(^nBu)_3$ at different temperatures.

Table VI. Second-Order Rate Constants and Activation Parameters for Ring-Expansion Reaction of $Fe(\eta^3\text{-}C_3Ph_3)(CO)_2(NO)$ (1a) with $P(^nBu)_3$ in Decalin

T (°C)	k_2 (s^{-1} M^{-1})	ΔH^* (kcal/mol)	ΔS^* (cal/mol·K)
69.5	4.62×10^{-4}		
81.5	4.62×10^{-4}		
91.0	1.57×10^{-3}	13.7 ± 1.8	−35.3 ± 5.4

Table VII. First-Order Rate Constants and Activation Parameters for CO Substitution Reaction of $Co(C_3Ph_3)(CO)_3$ (4) with $P(^nBu)_3$ in Toluene

T (°C)	k_1 (s^{-1})	ΔH^* (kcal/mol)	ΔS^* (cal/mol·K)
61.0	9.83×10^{-6}		
70.5	3.73×10^{-5}		
81.5	1.67×10^{-4}	31.9 ± 0.4	13.7 ± 1.4

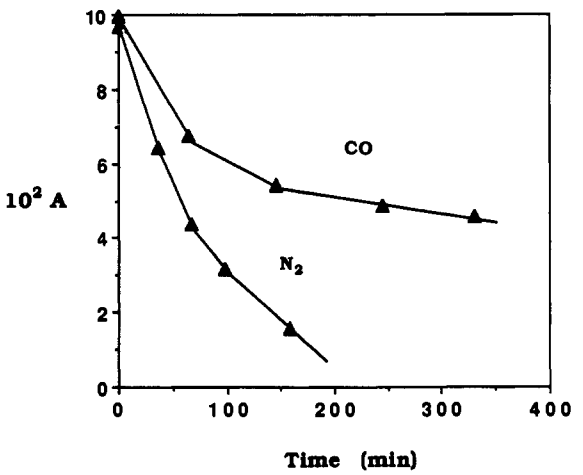

Figure 5. Plot of IR absorbance of CO stretching of $Co(\eta^3\text{-}C_3{}^tBu_3)(CO)_3$ (**6a**) vs time in the reactions with $P(OEt)_3$ (0.16 M) under N_2 or CO atmosphere at 90.6 °C.

Scheme I

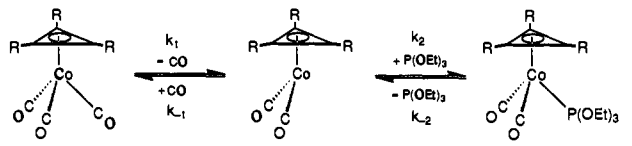

for the coordinatively unsaturated active intermediate (Scheme I). The proposed reaction mechanism (Scheme I) is also consistent with the fact that, under 1 atm of CO and at 0.16 M $P(OEt)_3$ ([complex] = 4×10^{-3} M), a plot of ln A_t vs time does not yield a straight line. The rate for the disappearance of reactant became slower as the concentration of the product increased (Figure 5). According to the reaction mechanism (Scheme I),

$$\ln(A_t - A_\infty) = \frac{k_1k_{-2}[CO] + k_1k_2[P(OEt)_3]}{k_{-1}[CO] + k_2[P(OEt)_3]}t + \text{constant}$$

A plot of $\ln(A_t - A_\infty)$ vs time shows a good linear coefficient (0.998), and k_{obsd} obtained from its slope is 2.12×10^{-4} s^{-1}. The same results were observed for the reaction of $Co(\eta^3\text{-}C_3{}^tBu_3)(CO)_3$ with $P(^nBu)_3$ (0.12 M) under N_2 at 101 °C (Figure 3), for which k_{obsd} was not obtained due to the uncertainty of [CO] during the reaction. Despite the differences of basicities[30] of these ligands, the reverse reactions increase with increasing the size of the entering ligands.

On the basis of this reaction mechanism, an experiment was designed to measure the equilibrium constants of the reactions (Scheme I). This was done by investigating the reactions under 0.1 atm of CO and at lower concentrations for the small ligands and higher concentrations for the large ligands. Despite large differences in the basicities of the ligands, the equilibrium constants increase with decreasing size of the ligands (Table II). A plot of ln K vs cone angles[30] of the ligands shows a good linear relationship between the two (Figure 6). The results imply that the stabilities of the monosubstituted complexes are predominantly determined by steric effects of the ligand, reflecting a very crowded space around the metal in this system. The large ligands PPh_3 or $P(c\text{-}C_6H_{11})_3$ do not react with the cobalt complex.

It is of interest to note that the dissociative CO substitution of $Rh(\eta^3\text{-}C_3{}^tBu_3)(CO)_3$ (**6b**) is much faster relative to the Co and Ir compounds than is the rate of associative CO substitution of $Rh(\eta^5\text{-}C_5H_5)(CO)_2$ relative to the Co and Ir counterparts. Furthermore, it is now possible for the first time to compare the rates of CO dissociation from a Co triad system with the relative rates of CO dissociation from other transition metal triads.

Results show (Table I) that for the compounds $M(\eta^3\text{-}C_3{}^tBu_3)(CO)_3$ (**6**; M = Co, Rh, Ir) the Co complex is the most inert toward substitution. This is mainly because of the stronger Co–CO bond compared with the M–CO bonds of the other two complexes. The activation enthalpy for the dissociation reaction of CO from the Co is about 9 kcal/mol higher than that for the Ir compound and about 12 kcal/mol higher than that for the Rh compound. This order of enthalpy of activation for M–CO dissociation correlates with the CO stretching frequencies which increase in the order Co < Ir < Rh (Table I), suggesting a decrease in M–CO π-back-bonding in this order and a decrease in M–CO bond strength.

Other examples that first-row elements of the late transition metals form stronger M–CO bonds are known for $M(CO)_5$ (M = Fe, Os)[16] and for $M(CO)_4$ (M = Ni, Pt)[18] (Table VIII). The point is that for late transition metal complexes, the 1st row metals form stronger M–C bonds than the 3rd row transition metals. Just the opposite order is known for early transition metal complexes $M(CO)_6$ (M = Cr, W)[19] and $(\eta^5\text{-}C_5H_5)M(CO)_4$ (M = V, Ta)[20] (Table VIII). This difference between the early and the late transition metals is believed due to the fact that the late transition metals have filled d-orbitals which are responsible for π-bonding that helps strengthen the M–CO bond. π-Back-bonding makes less of a contribution to the M–CO bond strengths of the early transition metal complexes, because they contain fewer d-orbital electrons which could make π-back-bonding less pronounced. It was suggested[17] that stabilization of the M–CO bond for the first-row metal was predominantly by π-bonding and the third-row metal system was largely by σ-bonding. This implies the first-row late transition metals owe their M–CO strength to strong π-bonding, whereas the third-row early transition metals owe theirs to strong σ-bonding. Detailed molecular orbital calculations[18] based on density functional theory to estimate the first CO ligand dissociation energy of $M(CO)_n$ for the three binary metal carbonyl triads $M(CO)_6$ (M = Cr, Mo, W), $M(CO)_5$ (M = Fe, Ru, Os), and $M(CO)_4$ (M = Ni, Pd, Pt) show that the repulsive four-electron two-orbital interactions between occupied orbitals on the metal center and the occupied σ_{CO} lone-pair orbitals on the carbonyl ligands considerably destabilize the M–CO bonds in $M(CO)_5$ and $M(CO)_4$ carbonyls of 4d and 5d transition metals. This destabilization is not expected in the early transition metal complexes.

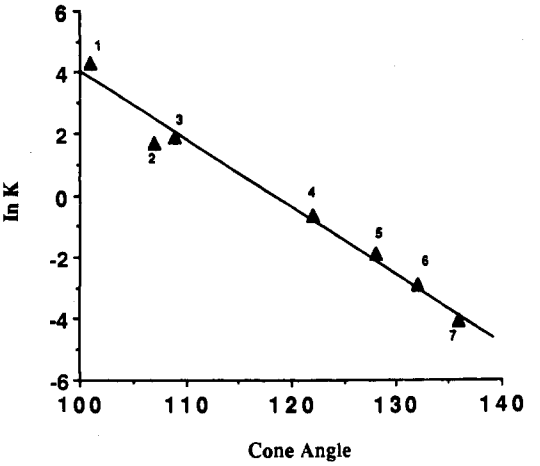

Figure 6. Plot of ln K for equilibrium reactions of $Co(\eta^3\text{-}C_3{}^tBu_3)(CO)_3$ (**6a**) with phosphine or phosphite ligands vs cone angles of the ligands. (See Table II for ligand numbers.)

Table VIII. Activation Enthalpies for CO Dissociation Reactions and CO Stretching Frequencies of First- and Third-Row Transition Metal Complexes

complex	ν_{CO} (cm^{-1})	ΔH^* (kcal/mol)
$Cp_2Ti(CO)_2$[a]	1973, 1895	26.9
$Cp_2Hf(CO)_2$	1967, 1874[b]	not available
$CpV(CO)_4$	1890, 1982[c]	35.3[d]
$CpTa(CO)_4$	1900, 2020[c]	45.8[e]
$Cr(CO)_6$[f]	1983	38.8
$W(CO)_6$[f]	1980	39.8
$Mn(CO)_5Cl$[g]	2070, 2016	27.5
$Re(CO)_5Cl$[h]	2056, 1987	27.3
$Fe(CO)_5$[i]	2023, 2001	40
$Os(CO)_5$[i]	2035, 1993	30.6
$Co(C_3{}^tBu_3)(CO)_3$	2046, 1976	34.4
$Ir(C_3{}^tBu_3)(CO)_3$	2053, 1986	25.9
$Ni(CO)_4$	1996[j]	24.9[k]
$Pt(CO)_4$	2052[j]	9.1[k]

[a] Reference 23. [b] Reference 24. [c] Reference 20. [d] Reference 26. [e] Reference 25. [f] Reference 19. [g] Reference 27. [h] Reference 28. [i] Reference 16; estimated value for $Fe(CO)_5$. [j] Reference 29. [k] Reference 18, first CO dissociation energies.

Kinetics and Mechanism of the CO Substitution Reaction of $Fe(\eta^3\text{-}C_3{}^tBu_3)(CO)_2(NO)$ (1b) with $P(^nBu)_3$. The reaction of

(18) Ziegler, T.; Tschinke, V.; Ursenbach, B. *J. Am. Chem. Soc.* **1987**, *109*, 4825.
(19) Angelici, R. J. *Organomet. Chem. Rev. A* **1968**, *3*, 173.
(20) Werner, R. P. M.; Filbey, A. H.; Manastyrsky, S. A. *Inorg. Chem.* **1964**, *3*, 298.

Scheme II

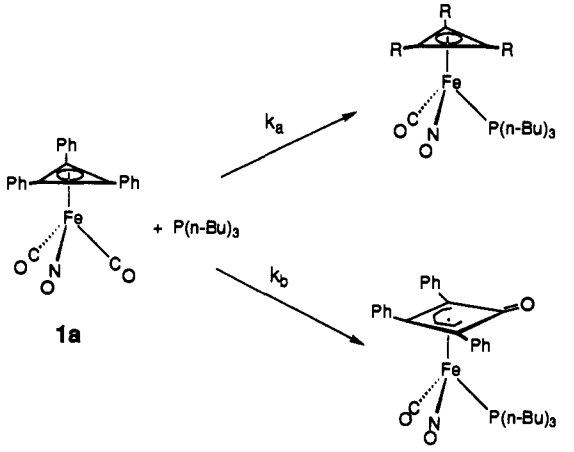

$Fe(\eta^3\text{-}C_3{}^tBu_3)(CO)_2(NO)$ with $P(^nBu)_3$ affords exclusively the monosubstituted complex (eq 3). The kinetics of this reaction (eq 3) obeys a two-term rate law (eq 4), which suggests the reaction occurs simultaneously by dissociative and associative pathways. It is well-known[7] that 18-electron metal nitrosyl complexes undergo CO substitution by an associative mechanism via an sp^2 bent-NO allowing a stable 18-electron active intermediate pathway. This associative reaction for the iron complex (eq 3) could proceed by an 18-electron transition state involving either a bent-NO or an $\eta^3 \rightarrow \eta^1$ ring-slippage mechanism. The bent-NO mechanism seems more likely, because the ring-slippage mechanism is known (see next section) to result in the formation of the oxocyclobutenyl product with ring-expansion and because the isoelectronic cobalt complex (see previous section) does not react by a parallel associative pathway.

Kinetics and Mechanism for the Reaction of $Fe(\eta^3\text{-}C_3Ph_3)(CO)_2(NO)$ (1a) with $P(^nBu)_3$. The reaction of $Fe(\eta^3\text{-}C_3Ph_3)(CO)_2(NO)$ with $P(^nBu)_3$ gives both CO substitution and ring-expansion products (eq 5), with the rate of disappearance of starting carbonyl following a two-term rate law (eq 4). Under the same experimental conditions, the reaction of $Fe(\eta^3\text{-}C_3Ph_3)(CO)_2(NO)$ with PPh_3 follows only a dissociative pathway to yield monosubstituted product with a rate constant the same as k_1 obtained from the reaction with $P(^nBu)_3$. The rate for dissociation of CO from the metal is faster for $Fe(\eta^3\text{-}C_3Ph_3)(CO)_2(NO)$ than for the analogous *tert*-butyl compound (Table IV). This is unexpected on the basis of steric factors, as the bulky *tert*-butyl groups should assist CO dissociation, but instead electronic effects seems to control the relative reactivities of these two complexes. Being an electron-withdrawing group, the phenyl substituents decrease electron density on the metal much more efficiently than does the electron-donating group *tert*-butyl. Thus the presence of phenyl groups decrease the electron density on Fe and as a result decrease the Fe to CO π-bonding. This is supported by the higher CO stretching frequencies of $Fe(\eta^3\text{-}C_3Ph_3)(CO)_2(NO)$ compared with $Fe(\eta^3\text{-}C_3{}^tBu_3)(CO)_2(NO)$. The activation energy for CO dissociation from $Fe(\eta^3\text{-}C_3Ph_3)(CO)_2(NO)$ is about 3 kcal/mol lower than that for $Fe(\eta^3\text{-}C_3{}^tBu_3)(CO)_2(NO)$ (Table IV) in agreement with the phenyl system having the weaker Fe–CO bond.

In order to obtain information on the formation of the monosubstituted product and the ring-expansion product, the distributions of the two products were determined at different phosphine concentrations. Assuming the two products are formed by two different reaction pathways (do not involve a common active intermediate), then $k_{obsd} = k_a + k_b$ (Scheme II). Since $C_4/C_3 = k_b/k_aI$ (C_4 and C_3 are the absorbances of CO stretching bands of the two complexes; I is the ratio of molecular absorptivities of the two complexes), $k_{obsd} = K\,C_4/C_3 + k_a$ ($K = Ik_a$); a plot of k_{obsd} vs C_4/C_3 should give a straight line, and the intercept of the line affords k_a (Figure 7). Table IX reports the relative distributions of products at different ligand concentrations for the reaction (eq 5). At 81.5 °C, $k_a = 6.30 \times 10^{-4}$, which is about the same as k_1 (5.95×10^{-4}, Table IV). This indicates that the substitution reactions occurs totally by a dissociative mechanism, while the ring expansion reaction is by an associative mechanism.

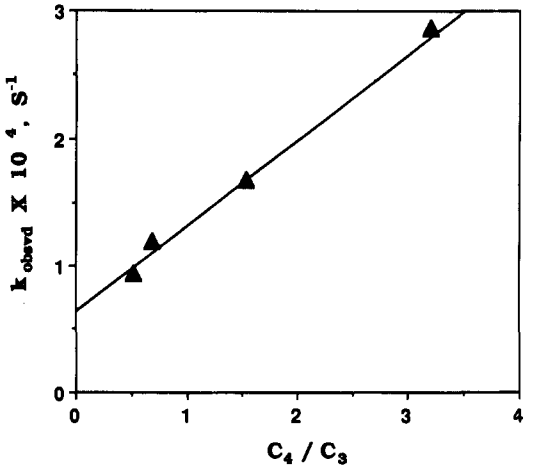

Figure 7. Plot of k_{obsd} vs distributions of ring-expansion and CO substitution products for the reaction of $Fe(C_3Ph_3)(CO)_2(NO)$ (**1a**) with $P(^nBu)_3$ at 81.5 °C.

Table IX. Relative Yields of Ring-Expansion and CO Substitution Products for the Reaction of $Fe(C_3Ph_3)(CO)_2(NO)$ (1a) with $P(^nBu)_3$ in Decalin

$[P(^nBu)_3]$ (M)	$C_4/C_3{}^a$	$[P(^nBu)_3]$ (M)	$C_4/C_3{}^a$
4.02×10^{-2}	0.523	1.34×10^{-1}	1.54
6.70×10^{-2}	0.686	2.68×10^{-1}	3.20

^{a} C_4 = absorbance of ring-expansion product at 1990 cm^{-1}; C_3 = absorbance of CO substitution product at 1958 cm^{-1}.

Compared with the *tert*-butyl analogue **1b**, the associative reaction for $Fe(\eta^3\text{-}C_3Ph_3)(CO)_2(NO)$ (**1a**) is a favorable pathway (Table IV). Considering the metal center in these complexes, there is less electron density on the metal atom and less steric crowding around the metal in $Fe(\eta^3\text{-}C_3Ph_3)(CO)_2(NO)$ than in the analogous *tert*-butyl complex. Thus $Fe(\eta^3\text{-}C_3Ph_3)(CO)_2(NO)$ should be more reactive than the *tert*-butyl complex toward nucleophilic attack via a bent-NO pathway. However, the less bulky phenyl group also makes it easier for an $\eta^3 \rightarrow \eta^1$ ring-slippage to occur than the bent-NO required by the *tert*-butyl system. That an η^1 intermediate is possible is supported by the X-ray structure determination of $Fe(\eta^5\text{-}C_5H_5)(\eta^1\text{-}C_3Ph_3)(CO)_2$.[8] Furthermore, this compound has been converted to the ring-expansion product photochemically.[8] Therefore, it is reasonable to suggest that the associative reaction involves an η^1 transition state/active intermediate (Scheme III, structure (a)), which then is followed by a well-recognition ligand migratory insertion type reaction.[21] This process is accompanied by the olefin coordination to Fe to form intermediate b, which in turn leads to the ring-expansion product. Although detailed mechanistic studies[22] on

(21) Collman, J. P.; Hegedus, L. S.; Norton, J. R.; Finke, R. G. *Principles and Applications of Organotransition Metal Chemistry*; University Science Books: Mill Valley, California 1987.
(22) Donaldson, W. A.; Hughes, R. P. *J. Am. Chem. Soc.* **1982**, *104*, 4846.
(23) Palmer, G. T.; Basolo, F.; Kool, L. B.; Rausch, M. D. *J. Am. Chem. Soc.* **1986**, *108*, 4417.
(24) Sikora, D. J.; Rausch, M. D. *J. Organomet. Chem.* **1984**, *276*, 21.
(25) Freeman, J.; Basolo, F. *Organometallics* **1991**, *10*, 256.
(26) Faber, G. C.; Angelici, R. J. *Inorg. Chem.* **1970**, *9*, 1586; **1984**, *23*, 4781.
(27) Angelici, R. J.; Basolo, F. *J. Am. Chem. Soc.* **1962**, *84*, 2495.
(28) Brown, D. A.; Sane, R. T. *J. Chem. Soc. A* **1971**, 2088.
(29) Kundig, E. P.; McIntosh, D.; Moskovits, M.; Ozin, G. A. *J. Am. Chem. Soc.* **1973**, *95*, 7234.
(30) (a) Tolman, C. A. *Chem. Rev.* **1977**, *77*, 313. (b) Rahman, M. M.; Liu, H. Y.; Eriks, K.; Prock, A.; Giering, W. P. *Organometallics* **1989**, *8*, 1.

Scheme III

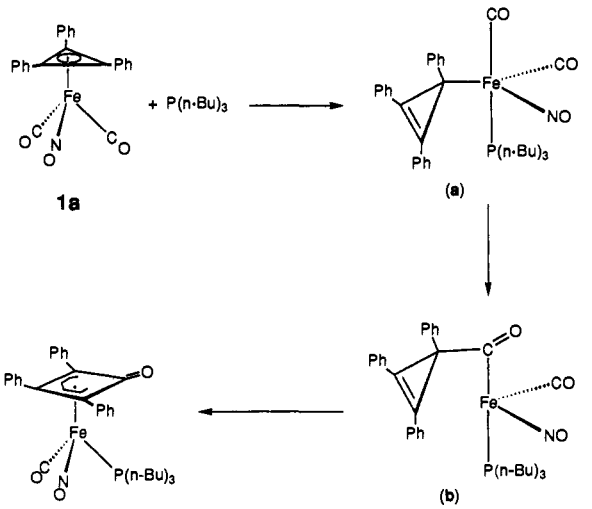

reactions of $[Co(CO)_4]^-$ with cyclopropenyl cations show that cleavage of the cyclopropene ring C–C bond does not directly involve a (η^1-cyclopropenyl)cobalt intermediate, structure type b has been identified to be the precursor of ring-expansion products.[22]

Kinetics and Mechanism for CO Substitutions of $Co(\eta^3\text{-}C_3Ph_3)(CO)_3$ (4) with $P(^nBu)_3$. Interestingly, reaction of $Co(\eta^3\text{-}C_3Ph_3)(CO)_3$ with $P(^nBu)_3$ only yields a monosubstituted product by a dissociative mechanism. The energy for CO dissociation from $Co(\eta^3\text{-}C_3Ph_3)(CO)_3$ is about 3 kcal/mol lower than that for the analogous *tert*-butyl complex. The Co–CO bond energy difference in these two complexes is about the same as that observed for Fe–CO in $Fe(\eta^3\text{-}C_3Ph_3)(CO)_2(NO)$ (**1a**) and $Fe(\eta^3\text{-}C_3{}^tBu_3)(CO)_2(NO)$ (**1b**). In fact, the CO dissociation energy for $Co(\eta^3\text{-}C_3Ph_3)(CO)_3$ is similar to that for the analogous iron complex. This suggests that the two complexes have similar electronic structure in the ground state, but it is not clear why this cobalt compound cannot undergo associative reaction while the analogous iron complex can.

Acknowledgment. We thank the National Science Foundation for the support of this research. J.K.S. thanks Northwestern University for a University Fellowship. R.P.H. is grateful to Johnson-Matthey Aesar/Alfa for a generous loan of precious metal salts.

Supplementary Material Available: Tables 1S–3S, listing actual values of k_{obsd} for the three different reactions investigated (3 pages). Ordering information is given on any current masthead page.